Agricultural and Forest Meteorology 310 (2021) 108634

Contents lists available at ScienceDirect

Agricultural and Forest Meteorology

journal homepage: www.elsevier.com/locate/agrformet

Tree-ring density and carbon isotope composition are early-warning signals of drought-induced mortality in the drought tolerant Canary Island pine

Rosana López [a,*], Francisco Javier Cano [b], Jesús Rodríguez-Calcerrada [a], Gabriel Sangüesa-Barreda [c], Antonio Gazol [d], J. Julio Camarero [d], Philippe Rozenberg [e], Luis Gil [a]

[a] Departamento de Sistemas Naturales e Historia Forestal, Universidad Politécnica de Madrid. Ciudad Universitaria, 28040 Madrid, Spain
[b] ARC Centre of Excellence for Translational Photosynthesis, Hawkesbury Institute for the Environment. Western Sydney University, Richmond, NSW 2753, Australia
[c] EiFAB-iuFOR, University of Valladolid, Campus Duques de Soria, 42004 Soria, Spain
[d] Instituto Pirenaico de Ecología (IPE-CSIC), Avda. Montañana 1005, E-50192 Zaragoza, Spain
[e] Biologie Intégrée pour la valorisation de la diversité des Arbres et de la Forêt" (BIOFORA, INRAE), 2163 Avenue de la Pomme de Pin, BP 20619, Ardon, 45166 Olivet Cedex, France

ARTICLE INFO

Keywords:
Dieback
Drought
Pinus canariensis
Tree-ring width, Water use efficiency
Wood density, Xylem functional anatomy

ABSTRACT

Tree death is not always preceded by a visible decline in vigor (canopy dieback) or a progressive loss in crown volume. Identifying early-warning signals of incipient decline can help to implement the necessary measures to prevent tree death. The aim of this work is to understand what functional alterations preceded the massive drought-induced death of adult *Pinus canariensis* trees in an arid stand, located in the Canary Islands. To this aim, we analyzed interannual variations in earlywood and latewood width, wood density and anatomy, and carbon isotope composition, and the relationships among these variables, in dead and living trees from 1980 to 2013. Dead trees grew less since the 1990′s, produced fewer parenchyma rays and resin canals, and exhibited a trend of decreasing latewood density and a marked shift in carbon isotope discrimination over the last 34 years that were reversed in living trees. Higher wood density in living trees resulted from thicker tracheid cell walls rather than narrower lumens. The intrinsic water use efficiency shifted from higher to lower values in dead trees after the 2000s. These results suggest a carbon limitation to maintain hydraulic safety under xylem tension, as well as to maintain storage and defense capacity, which can render trees more vulnerable to severe drought episodes. A long-term trend of decreasing tree-ring density and a reduced intrinsic water use efficiency in the short-term can be early-warning signals of carbon limitation and tree decline in drought-stressed *P. canariensis*. The analysis of these variables can be used to assess tree decline risks in similarly vulnerable conifer populations inhabiting drought-prone regions.

1. Introduction

Episodes of drought-induced forest dieback and mortality have been observed in the last decades worldwide (Allen et al., 2010; Rodríguez-Calcerrada et al., 2017a), and are likely to become more frequent in the future as a consequence of increasing aridity and rising temperature (Allen et al., 2015; Dai, 2013). Strong efforts to reveal the mechanisms underlying forest dieback and associated tree mortality have been made in the last decade, particularly following the framework suggested by McDowell et al. (2008), in which an interdependent set of processes concerning carbon storage depletion and plant hydraulics are involved. Recent evidence points to the failure of the plant hydraulic system as the ubiquitous mechanism of mortality across taxa (Adams et al., 2017; Choat et al., 2018). However, in gymnosperms some cases have been observed where carbon balance and water transport were both compromised (Adams et al., 2017; Garcia-Forner et al., 2016).

Many studies concerning the mechanisms of tree mortality have used potted plants (e.g. saplings) where drought is imposed at higher rates than in natural conditions, and the root system is constrained (Mitchell et al., 2014; Rodríguez-Calcerrada et al., 2017b; Sevanto et al., 2014). Large trees in natural conditions are more resistant and resilient to drought; however, their height, and irregular branch mortality upon drought limit the applicability of many physiological measurements. Dendroecological studies comparing wood traits of dead and living trees

* Corresponding author
E-mail address: rosana.lopez@upm.es (R. López).

https://doi.org/10.1016/j.agrformet.2021.108634
Received 4 October 2020; Received in revised form 27 June 2021; Accepted 30 August 2021
Available online 14 September 2021

of similar age and size, and growing in the same conditions have shown promising to unveil the process of mortality under drought, particularly when they include hydraulics and functional traits such as wood density, wood anatomy, or wood stable isotope ratios (Camarero et al., 2015a, 2015b; Martínez-Vilalta, 2018). These studies provide an integral, comprehensive, long-term retrospective analysis of tree responses to environmental changes, and allow for the possibility to work with mature trees usually underrepresented in studies of tree mortality (Choat et al., 2018; Gessler et al., 2018).

Radial growth of the woody stem is a highly integrative process influenced by whole tree physiology, and regulated by environmental conditions (Fonti et al., 2010; Martínez-Vilalta, 2018). It is commonly observed that acute, short-term stressors such as extreme droughts trigger a decrease in radial growth rates that last for several years to decades prior to death (DeSoto et al., 2020; Hereş et al., 2012; Linares and Camarero, 2012; Staley, 1965). Cailleret et al. (2017) associated this long-term decrease in growth to a gradual decline in carbon reserves coupled with a gradual hydraulic dysfunction. Nevertheless, there are exceptions in which dying trees only experienced growth reductions a few years before death (Bigler and Veblen, 2009; Voltas et al., 2013; Zadworny et al., 2019), associated with generalized hydraulic failure or bark beetle attacks (Cailleret et al., 2017).

The xylem of gymnosperms is mainly composed of tracheids, which provide mechanical support and define water transport capacity (Tyree and Zimmermann, 2002). Prevalence of one function over the other is determined by changes in lumen area and wall thickness of these cells. At the beginning of the growing season, earlywood tracheids have relatively large lumens and thinner walls, and are thus optimized to supply water to the canopy. Whereas, latewood formed later in the growing season is characterized by tracheids with smaller lumens and thicker walls, less efficient conducting water, but mechanically stronger (Pellizzari et al., 2016; Domec and Gartner, 2002; Tyree and Zimmermann, 2002). The mechanical properties of the tracheids are related to the thickness-to-span ratio (i.e. the ratio of tracheid double wall thickness to lumen diameter; Sperry et al., 2006). Because this ratio provides an indirect assessment of hydraulic safety against xylem implosion (Hacke et al., 2006), latewood and in general denser woods are considered to be more resistant to cell implosion under water tension than earlywood and woods with lower density (Hacke and Sperry, 2001). Parenchymatic rays and resin canals are responsible of the storage and defense functions of the xylem (Tyree and Zimmermann, 2002). The variable investment of carbon and mineral nutrients between earlywood tracheids, latewood tracheids or parenchyma cells represents a dynamic way to guarantee xylem water supply, defense, and storage functions under fluctuating environmental conditions (Sass-Klaassen et al., 2016). Sustained or acute stresses, however, can cause an unbalance among these functions and jeopardize tree vigor in the long run.

Besides these anatomical proxies of xylem functions, carbon isotope composition ($\delta^{13}C$) of tree rings provides additional insights into the tree water and carbon economy (Gessler et al., 2018). Specifically, the carbon isotope discrimination ($\Delta^{13}C$), which accounts for the discrimination against the ^{13}C isotope made by the plant with respect to the $\delta^{13}C$ of CO_2 in the air, has been extensively used to quantify the intrinsic water-use efficiency (iWUE), i.e. the ratio of net photosynthesis to stomatal conductance to water vapor (Francey and Farquhar, 1982; Seibt et al., 2008). In Mediterranean species, the variation in iWUE from year to year has been usually explained by climatic constraints, mainly drought (Ferrio and Voltas, 2005; Granda et al., 2014) as stomatal conductance decreases to reduce water loss (Battipaglia et al., 2013) and avoid the development of high xylem tensions.

Some populations of Mediterranean pines located at the dry edges of their distribution limit are likely to be particularly vulnerable to increase drought severity (Camarero et al., 2015a; Hampe and Petit, 2005; Sánchez-Salguero et al., 2017). In 2013, after two consecutive extremely dry years, a massive mortality event in a *Pinus canariensis* Chr. Sm. Ex DC plantation (Fig. S1) was recorded by the Forestry Service at the South of Gran Canaria (Canary Islands, Spain). In previous studies, trees from this area showed high embolism resistance (López et al., 2013), distinctive sclerophyllous leaves (López et al., 2008), and some degree of plasticity in these traits, associated with survival under dry conditions (López et al., 2007, 2010, 2016).

We tested the following hypotheses to explain the widespread mortality event of 2013: 1) now-dead trees (dead trees hereafter) show a gradual decrease in radial growth rates for decades prior to death in comparison with living trees; 2) dead trees are more vulnerable to xylem dysfunction than surviving ones due to reduced carbon investment in the xylem (i.e. narrow tree rings of low density); 3) phenotypic integration of xylem traits differs between dead and living trees; that is, dead trees show stronger trade-offs between hydraulic efficiency and safety, and between iWUE and wood density that predispose these plants to die. To test these hypotheses, we investigated changes in radial growth (tree-ring width), wood density, anatomy (i.e. lumen area and cell-wall thickness), and iWUE derived from $\Delta^{13}C$ from 1980 to 2013. We also assessed the relationships of these variables among them and with the local climate trend. Our specific objectives were to: i) shed light on the mechanisms underpinning tree mortality after an extreme drought event, ii) identify differences in the phenotypic integration of xylem traits related to water transport, defense, storage and mechanical support between living and dead trees; and iii) facilitate interpretations of climate control over these traits.

2. Material and methods

2.1. Study site, sampling strategy and plant material

We selected a *Pinus canariensis* reforested stand located in Tirajana, south of Gran Canaria, Spain (27° 54′ N, 15° 37′ W, 1100–1200 m a.s.l.), affected by extensive tree mortality in 2013 (ca. 35% of dead trees; Fig. S1). The site has an arid environment, with mean annual precipitation 196 mm, mean annual temperature 17.7 °C and ca. 8 months of drought (average data from 1950 to present). Soils are shallow, very compact and stony.

We chose 24 dominant adult trees that died during 2013. Needles of dead trees have dried out and dropped at sampling time. After felling each tree, a wood slice was obtained at breast height (1.3 m). We also selected the nearest dominant living tree (24 living trees in total), and extracted two wood cores at 1.3 m using 5.15 mm-diameter increment borers. Wood samples were collected between January and March 2014. We measured the diameter at breast height (dbh, 1.3 m) of all sampled trees and counted the rings from bark to pith to estimate their age at 1.3 m. All the slices and cores were dried at room temperature. One core of each living tree and a piece of 1–3 cm width of the slice of the dead trees were transported to the INRAE (formerly INRA, Orléans, France) for analysis of tree-ring width, wood density and anatomy. The remaining material was sent to IPE-CSIC (Zaragoza, Spain) for verifying the previous cross-dating, and sample preparation for isotope analysis. Living and dead trees did not significantly differ in dbh (average dbh 14.9 ± 0.5 cm) or age (53 ± 1.3 years).

Climate data from 1980 to 2013 were obtained from Climate Explorer, E-OBS temperature and precipitation datasets (https://climexp.knmi.nl/start.cgi).

2.2. Growth and microdensity profiles

Wood slices and cores were sawn to 2–2.5 mm thickness. After resin extraction with pentane during two days, samples were analyzed by indirect X-ray densitometry (Polge, 1966). X-ray films were scanned at a 1000 dpi resolution, with 8 bits depth per pixel. Images were processed with WinDendro (Regent Instruments Inc.) to obtain the density profiles from which tree-ring width was measured as described in Martinez-Meier et al. (2008).

Trees were visually cross-dated and microdensity variables were

computed yearly from 1980 to 2013 rings. We described each of the tree-rings of this period with nine descriptors: ring width (RW), earlywood width (EW), latewood width (LW), latewood proportion (LW%), mean ring density (D), minimum ring density (D_{min}), maximum ring density (D_{max}), earlywood density (ED) and latewood density (LD). Earlywood and latewood densities were taken as the average density of their respective ring portion (Martínez-Meier et al., 2008). Some trees were younger than the average (53 years) and we discarded them from further analysis. In total we successfully dated and measured 21 living trees and 20 dead trees.

2.3. Wood anatomy

Five cores of living trees and five slices of dead trees used for growth and microdensity measurements were randomly selected for the anatomical study. Wood samples were prepared for light microscopy observation following standard protocols (Rodríguez-García et al., 2016). Transversal sections 15–25 μm thick were cut using a sliding microtome (Leica SM 2400) and stained with a solution of 1% safranin. Then sections were mounted and digitalized with a camera attached to a light microscope (Olympus BX50) for further image analysis with ImageJ (Schneider et al., 2012). All variables were measured or calculated on a per tree-ring basis, separately for earlywood and latewood. For each ring, lumen area (*A*), tangential lumen diameter (*b*) and double cell wall thickness (*t*) were measured in at least 120 tracheids in the earlywood and 70 tracheids in the latewood. Tracheids were measured along complete radial rows to include a representative estimate of ring anatomical variability. Tracheid separation was aided by the 'Watershed' function in ImageJ and, when necessary, by manually drawing tracheid borders. The equivalent circular lumen diameter (*D*) was calculated from the tracheid lumen area. The mean hydraulic diameter (*Dh*) was used as a proxy of hydraulic efficiency, and it was calculated following Tyree and Zimmermann (2002) as:

$$Dh = \left(\frac{\sum D^4}{N}\right)^{0.25} \quad (1)$$

where *Dh* is the hydraulic diameter, *D* is the equivalent circular lumen diameter, and *N* is the number of tracheids.

The $(t/b)^2$ ratio or cell wall reinforcement has been related to resistance to implosion and correlates with drought embolism resistance across species (Hacke et al., 2001), but not within the annual ring (Dalla-Salda et al., 2014). Moreover, we considered the percentage of xylem area occupied by cell walls (%t) determined in the cross sectional area, as a proxy of carbon cost. Finally, the number of parenchyma rays (PR) and axial resin canals (RC) were counted per growth ring and expressed per ring area (ring width x core diameter). See Table 1 for a complete list of all analyzed traits.

2.4. Stable carbon isotope composition ($\delta^{13}C$) and intrinsic water use efficiency (iWUE)

The same ten trees (five living and five dead) used for anatomical measurements were selected for carbon isotope analysis. For each wood core and each slice, rings were separated in 5-year tree-ring groups using scalpels. The resulting wood samples were ground to a fine powder using a ball mixer mill (Retsch Mixer MM301, Leeds, UK). A subsample of the homogenized powder was weighed and introduced into tin foil capsules and sent to the Stable Isotope Facility of the University of California, Davis, USA. $\delta^{13}C_{wood}$ was measured using an isotope-ratio mass spectrometer (Thermo Finnigan MAT 251, Bremen, Germany) interfaced with a Flash EA-1112 elemental analyzer. The relationship between stable isotopes ^{13}C and ^{12}C was expressed in relation to a Pee-Dee Belemnite (PDB) standard. The accuracy of $\delta^{13}C_{wood}$ measurements was ±0.05‰.

Carbon isotope discrimination was calculated following Farquhar and Richards (1984):

$$\Delta^{13}C_{needle}\ (‰) = \left(\frac{\delta^{13}C_{air}(‰) - \delta^{13}C_{needle}(‰)}{\frac{\delta^{13}C_{needle}(‰)}{1000} + 1}\right) \quad (2)$$

Because the analyses were made on 5- ring groups, we used averaged values of $\delta^{13}C_{air}$ for each 5–year time period from freely available data (ftp://aftp.cmdl.noaa.gov/data/trace_gasses/co2c13/flask/) collected at Izaña, Tenerife, Canary Islands, Spain (28°18′ N, 16°29′ W, 2373 m a.s.l.), and analyzed by NOAA ESRL Carbon Cycle Cooperative Global Air Sampling Network over 1990–2014 (White, Vaughn & Michel, 2015); $\delta^{13}C_{air}$ values were then linearly extrapolated back to 1982. To extrapolate tree-ring $\delta^{13}C$ data to pine needles, we applied the correction: $\delta^{13}C_{needle}(‰) = \delta^{13}C_{wood}(‰) - 2(‰)$, according to previous results where $\delta^{13}C_{wood}$ was 2‰ less negative than that of the needles in *Lagarostrobos franklinii* (Francey et al., 1985).

The intrinsic water use efficiency (iWUE, in μmol CO_2 mol^{-1} H_2O) was calculated following the simplified model of ^{13}C discrimination of Farquhar et al. (1982):

$$iWUE_{needle} = \frac{C_a}{1.6}\left(\frac{b - \Delta^{13}C_{needle}}{b - a}\right) \quad (3)$$

where *a* is the fractionation during CO_2 diffusion through the stomata (4.4‰; O'Leary, 1981), *b* is the net fractionation associated to carboxylation by Rubisco and PEP carboxylase (27.3‰; Evans et al., 1986), and C_a is the CO_2 concentration of the atmosphere averaged for each period

Table 1
List of traits included in the study, with abbreviations and units.

Abbreviation	Trait	Xylem function proxy	Units
Growth traits			
RW	Ring width		mm
EW	Earlywood width		mm
LW	Latewood width		mm
LW%	Latewood proportion		%
Wood density traits			
D	Wood density	Support	kg m^{-3}
D_{min}	Minimum ring density	Support	kg m^{-3}
D_{max}	Maximum ring density	Support	kg m^{-3}
ED	Earlywood density	Support	kg m^{-3}
LD	Latewood density	Support	kg m^{-3}
Anatomical traits			
Et	Earlywood double wall thickness	Support/Safety	μm
Lt	Latewood double wall thickness	Support/Safety	μm
b	Tracheid tangential lumen diameter	Efficiency	μm
$E(t/b)^2$	Earlywood cell wall reinforcement	Safety	
$L(t/b)^2$	Latewood cell wall reinforcement	Safety	
E%t	Cell wall proportion in earlywood	Support	%
L%t	Cell wall proportion in latewood	Support	%
EDh	Earlywood hydraulic diameter	Efficiency	μm
LDh	Latewood hydraulic diameter	Efficiency	μm
PR	Parenchyma ray density	Storage	Number mm^{-2}
RC	Resin canal density	Defense	Number mm^{-2}
^{13}C isotope composition traits			
$\delta^{13}C$	Carbon isotope composition		‰
$\Delta^{13}C$	Carbon isotope discrimination		‰
iWUE	Intrinsic water use efficiency		μmol CO_2 mol^{-1} H_2O

of five years from the freely available data (https://doi.org/10.15138/wkgj-f215) collected at Izaña, and analyzed by NOAA ESRL Carbon Cycle Cooperative Global Air Sampling Network, 1968–2018, Version: 2019–07 (Dlugokencky et al., 2019).

A sensitivity analysis to evaluate the effect of $\delta^{13}C_{air}$ and C_a on $iWUE_{needle}$ was also carried out.

2.5. Statistical analyses

We used generalized additive mixed models (GAMM; Wood, 2017) to evaluate if temporal trends in wood traits differed between living and dead trees. Separated models were created for RW, EW, LW, D, ED and LD. Tree identity was regarded as random factor since tree-rings represent repeated measures over the same individual. Thin-plate regression splines were used to model fixed effects (Wood, 2003). As fixed factors, we included the calendar year to account for the temporal trend, and the estimated tree age to represent the impact of ontogeny on tree growth. Further, a vitality factor classifying trees in living and dead was included to represent differences between the two groups. We also included the temperature of October in the year of tree-ring formation, as it showed a strong correlation with RW. We included interactions between calendar year and vitality, to account for the potential differences in growth trajectories between living and dead trees, and between the temperature of October and vitality to account for the potential different responses to climate. A first-order autocorrelation structure (AR1) was included to account for the dependency of the values in the year t from that in the year t-1. Several potential models were compared and the most parsimonious was selected according to the second-order Akaike Information Criterion (AICc), taking into consideration both parsimony and likelihood (i.e. the model with the fewest predictor variables for which the difference in AICc relative to minimum AICc is lower than 2; Burnham and Anderson, 2002).

The effect of vitality and calendar year on variables related to wood anatomy and carbon isotope discrimination were tested using repeated measurements ANOVA. Finally, to assess if phenotypic integration differed between earlywood and latewood, and living and dead trees, linear regression and Pearson correlation analyses were performed between variables related with growth, wood density, anatomy, and climate of the year of ring formation and the previous year (mean annual precipitation, precipitation in spring, summer, autumn and winter, mean annual temperature, mean temperature in spring, summer, autumn and winter). Bivariate relationships between traits were also assessed using simple linear or nonlinear least squares regression. We averaged values of these variables for the same 5-year time period than for $\Delta^{13}C$ to calculate the correlation coefficients.

All statistical analyses were performed using the R software (R Core Team, 2019). The "mgcv" package (Wood, 2017) was used to fit GAMM's.

3. Results

3.1. Radial growth, wood density and wood anatomy – trends in living and dead trees

Average ring width (RW) was 1.2 ± 0.1 mm (mean ± SE) in living trees and 0.9 ± 0.1 mm in dead trees, and significantly differed between living and dead trees from the 1990's (Fig. 1a). In dead trees, RW showed a significant negative trend from 1980 to 2012, whereas no trend was found for living trees during the same period (Fig. 1a; Table 2). The latewood proportion (LW%) significantly increased with time. It was lower than 19% at the beginning of the time series and higher than 22% at the end, and with no differences between living and dead trees due to two different patterns: in living trees, LW significantly increased with time whereas EW did not show any trend, while in dead trees EW showed a steeper decrease than LW (Fig. 1). Latewood density (LD) and D_{max} significantly increased over time in living trees, but they significantly decreased in dead trees (Fig. 2). Minimum wood density (D_{min}) was on average 0.51 g cm^{-3}, with no differences between living and dead trees, and no significant trend over time. The models proposed showed divergences between living and dead trees in all the ring-width variables (RW, EW and LW) and LD (Table 2 and Figs. S3, S4). However, the fraction of variation explained by the models was rather low and did not exceed 15% in any case.

We found a weak but significant temporal trend in traits related with cell wall measurements and parenchyma rays but not in those related with tracheid lumens (Fig. 3). Cell wall thickness (t) and area occupied by cell walls (%t) tended to increase slightly over time in the earlywood of dead and living trees (Fig. 3c, 3g). This was also true for latewood in living trees, but the trend was reversed in dead trees (Fig. 3d, 3h). Parenchyma rays (PR) significantly decreased with time from almost 7.0 rays mm^{-2} at the beginning of the study to less than 5.5 rays mm^{-2} in the last year (Fig. 3j). This decrease was more evident in dead trees from 1997 onwards (Fig. 3j). The number of resin canals was higher in living than in dead trees and tended to decrease over time (Fig. 3i).

Living trees formed significantly thicker cell walls and more parenchyma rays, and showed higher $(t/b)^2$ and %t than dead trees. Differences were significant in both earlywood and latewood (Fig. 3). By contrast, the mean hydraulic diameter (Dh), related to water transport efficiency, showed a clear interannual variability, and did not differ between dead and living trees for either earlywood or latewood (Fig. 3a, 3b).

3.2. $\delta^{13}C_{wood}$ and intrinsic water use efficiency (iWUE) – trends in living and dead trees

The analysis of $\delta^{13}C_{wood}$ revealed a similar $\delta^{13}C_{wood}$ in both living and dead trees during the first period analyzed (1982–1986) (Fig. 4; Table 3). The following period (1987–1991) was wetter and living trees showed a sharper decrease in $\delta^{13}C_{wood}$ than dead trees. Thereafter, $\delta^{13}C_{wood}$ showed a slight constant trend to decrease in both dead and living trees until 1997–2001, when $\delta^{13}C_{wood}$ suddenly dropped in dead trees (Fig. 4a; Table 3).

The two contrasting trends of living and dead trees became more evident when comparing the carbon isotope discrimination estimated in needles ($\Delta^{13}C_{needle}$), once the actual trends in $[CO_2]$ and $\delta^{13}C$ in the air were accounted for (Fig. 4b).

The estimated values of iWUE were highly influenced by the temporal changes in air $[CO_2]$ and $\delta^{13}C_{air}$ (Fig. S5). When these changes were taken into account, the iWUE of living trees exhibited a continuous increase from 1989 (Fig. 4c, Table 3), mainly due to the increase in air $[CO_2]$, rather than to the less negative $\delta^{13}C_{air}$ (Fig. S5). Dead trees showed significantly higher iWUE than living trees from 1987 to 1996, but in the driest period 1997–2001, there was a change in the tendency, and iWUE of dead trees started to decrease, while iWUE of living trees continued increasing. In the five years preceding the death of these trees, iWUE was significantly lower than in surviving trees (Fig. 4c, Table 3).

3.3. Phenotypic integration of xylem traits in living and dead trees

The correlation analyses supported that phenotypic integration differed between earlywood and latewood and between living and dead trees; still, some common patterns emerged (Fig. 5). A negative trade-off between hydraulic efficiency and safety existed except for the earlywood of living trees. Hydraulic safety was always positively correlated with mechanical support, and growth was always positively correlated with defense traits (Fig. 5). The number of significant correlations was higher in the latewood of living trees and in the earlywood of dead trees. In the former, $L(t/b)^2$ and RC were positively correlated and showed the highest number of significant correlations with other variables. In dead trees, EW was negatively correlated with ED and $E(t/b)^2$ and positively with EDh, RC and PR (Fig. 5).

Cell wall thickness and the area occupied by walls rather than lumen

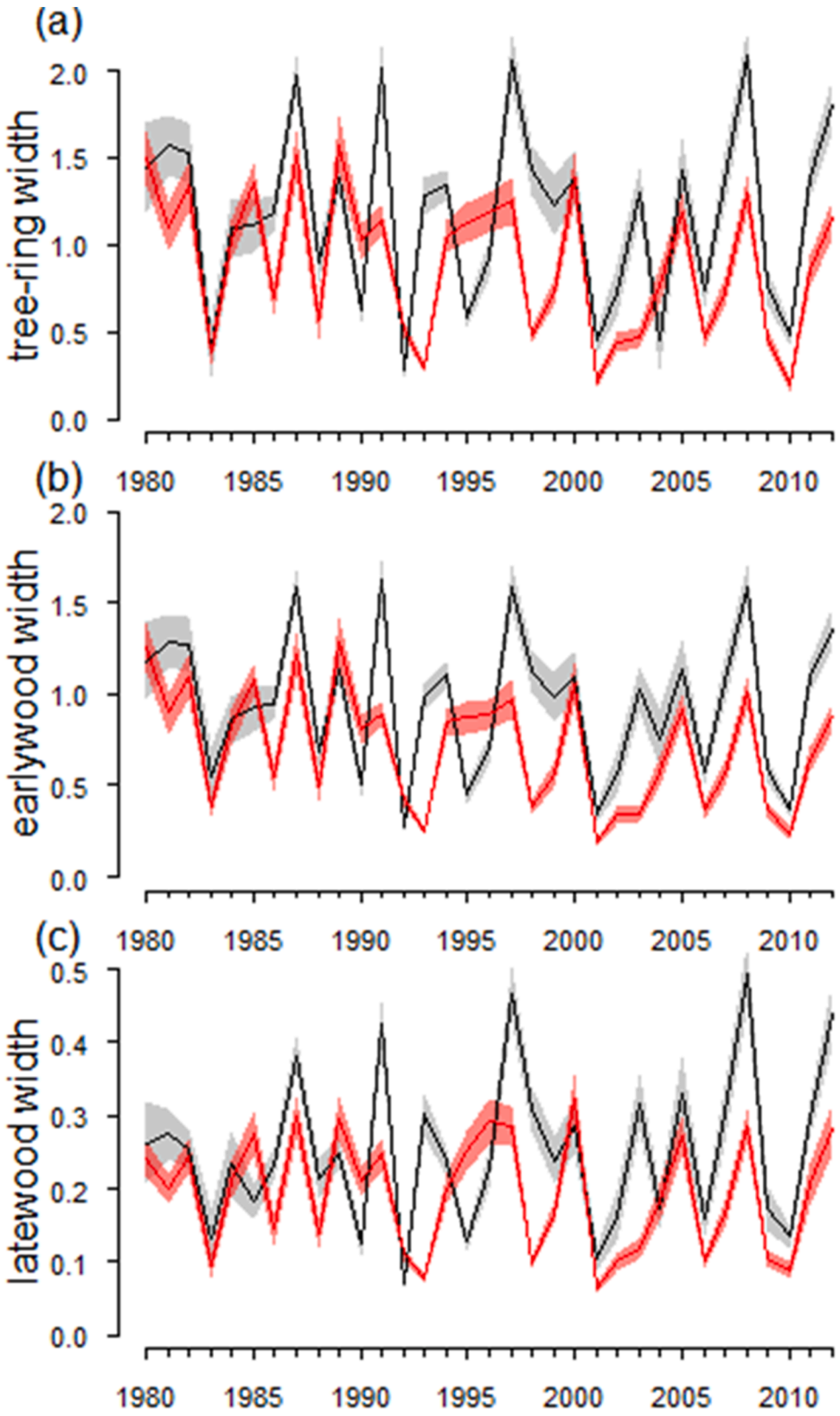

Fig. 1. Annual growth ring parameters (in mm). The lines represent mean observed values for living (black) or dead (red) trees. Polygons surrounding the lines represent the standard error. (For interpretation of the references to colour in this figure legend, the reader is referred to the web version of this article.)

Table 2
Variables included in the proposed models to explain wood formation in *P. canariensis*. For variables year, tree status (living or dead), tree age and the temperature in the year of the growth ring formation ($T_{october}$) and their interactions (columns) modelled with thin-plate regression splines, the F statistic of the variables (rows) and the expected degrees of freedom are shown. For those variables modeled as linear terms, the estimated regression coefficient () is shown. RW: ring width, EW: earlywood width, LW: latewood width, D: wood density, ED: earlywood density, LW: latewood density. Significant effects are indicated with * (p. < 0.1) and ** (p. < 0.01). See Table S1 for information of the competing models tested.

	RW	EW	LW	D	ED	LD
Year				76.91** (1.00)	73.09** (1.00)	
Year x living	0.14 (1.00)	1.68 (1.70)	9.43** (1.00)			13.98** (1.00)
Year x dead	20.72** (1.00)	28.00** (1.00)	2.02 (1.00)			1.90 (1.00)
Tree age	2.04 (1.00)	2.37 (1.00)	2.27 (1.00)	1.44 (1.00)		0.18 (0.67)
Status (living)	0.36 (± 0.12)**	0.31 (± 0.09)**	0.08 (± 0.02)**			0.05 (± 0.01)**
$T_{october}$	−0.08 (± 0.02)**	−0.07 (± 0.01)**	−0.02 (± 0.00)**	0.002 (± 0.001)**		−0.003 (± 0.002)
$T_{october}$ x status						
R^2	0.08	0.10	0.06	0.06	0.05	0.13

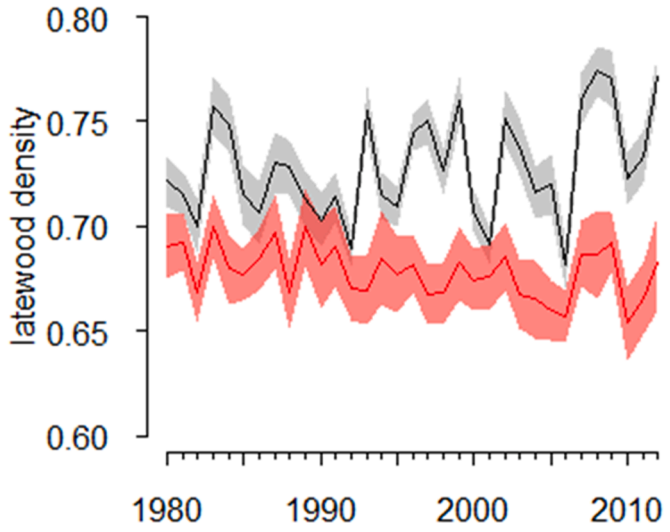

Fig. 2. Latewood density values (in g cm^{-3}). The lines represent observed values for living (black lines) or dead (red lines) trees. Polygons surrounding the lines represent the standard error. (For interpretation of the references to colour in this figure legend, the reader is referred to the web version of this article.)

area drove the variations in D, ED and LD (Fig. 6); this was particularly evident for LD (Fig. 6d; 6 h). Ring width (RW) in living trees was not correlated with D but showed a positive correlation with D_{max} and LD, and a negative correlation with D_{min} and ED (Table S2). In dead trees, however, RW was negatively correlated with all parameters of wood density (Table S2). $\Delta^{13}C_{needle}$ was positively correlated with ED, LD, $L(t/b)^2$ and L%t in living trees, but negatively correlated with LW and LD in dead trees (Fig. 7).

3.4. Influence of climatic conditions on growth, wood density and wood anatomy

From 1960 to 2013, there was a mean annual temperature increase of 2 °C at Tirajana ($r^2 = 0.52$), but no trend in mean annual precipitation, with a reference value of 180 mm $year^{-1}$ (Fig. S2). The decade from 1992 to 2001 was particularly dry with mean annual precipitation lower than 150 mm in all but two years, and mean annual temperatures ca. 0.5 °C higher than the average (Fig. S2). The next years were more humid and there was only two consecutive years, 2011 and 2012, with annual precipitation lower than 150 mm. From March 2011 to August 2012 the site received ca. 100 mm of rainfall. Moreover, the summer of 2012 was particularly warm, with mean monthly temperatures 1.5 °C higher than the average. Thus, the severe drought period of 2011–2012 was immediately followed by a marked heat wave in the summer of 2012.

Ring width and earlywood traits were more influenced by winter precipitation of the previous year in living trees and by current-year spring precipitation and temperature in dead trees, (Table S3), besides the positive correlation of October temperature in RW in both living and dead trees. Latewood traits were related to spring and summer precipitation in living trees and with autumn precipitation in dead trees.

In living trees winter precipitation of the previous year was positively correlated with RW, EW, PR, and Edh and negatively with $E(t/b)^2$ and E%t (Table S3). Spring precipitation was positively correlated with LDh but negatively with %LW, whereas summer precipitation was positively related with Lt and $L(t/b)^2$. Higher temperatures during spring were negatively correlated with PR and positively correlated with L%t (Table S3). Dead trees were mainly affected by spring climatic conditions: spring precipitation was positively related with RW and EW but negatively with %LW. Spring temperature was positively related with ED and %LW, but negatively with LD, D_{max}, RC and PR. Autumn precipitation was associated with higher LDh and lower LD and D_{max} (Table S3).

4. Discussion

Pinus canarienis has the southernmost distribution limit of its natural range in the southern part of Gran Canaria, where survival and natural regeneration are severely constrained by water availability (López de Heredia et al., 2014). Approximately 35% of planted *P. canariensis* trees died in 2013 in this area, after the severe drought in 2011–2012. Our results suggest that trees succumbed following decades of carbon limitation after the 1990s drought, which appeared to affect stomatal regulation, xylem embolism resistance and storage and defense capacity. These results agree with a recent study showing that gymnosperms surviving a severe drought recovered better from previous non-lethal droughts than dying trees (DeSoto et al., 2020); also with observations of loss of resilience after multiple droughts (Bose et al., 2020). Here we discuss the interdependence of hydraulic dysfunction and carbon limitation underpinning drought-induced death of *Pinus canariensis*, which can be extensible to other tree species in marginal climate populations (McDowell, 2011).

4.1. Decreasing wood density, iWUE and growth warn of upcoming tree death after prolonged drought

Extremely dry conditions in the studied area resulted in low growth rates in both dead and living trees. Growth of dead trees was even lower in the years prior to death (i.e. 1990 onwards; Fig. 1). Trugman et al. (2018) applied the optimal carbon allocation theory to explain this widely observed multi-year lag in post-drought mortality. If during prolonged or severe droughts the water transport capacity of the tree is constrained by massive embolism in the hydraulic system, the only way to recover water transport and ensure carbon uptake in the absence of

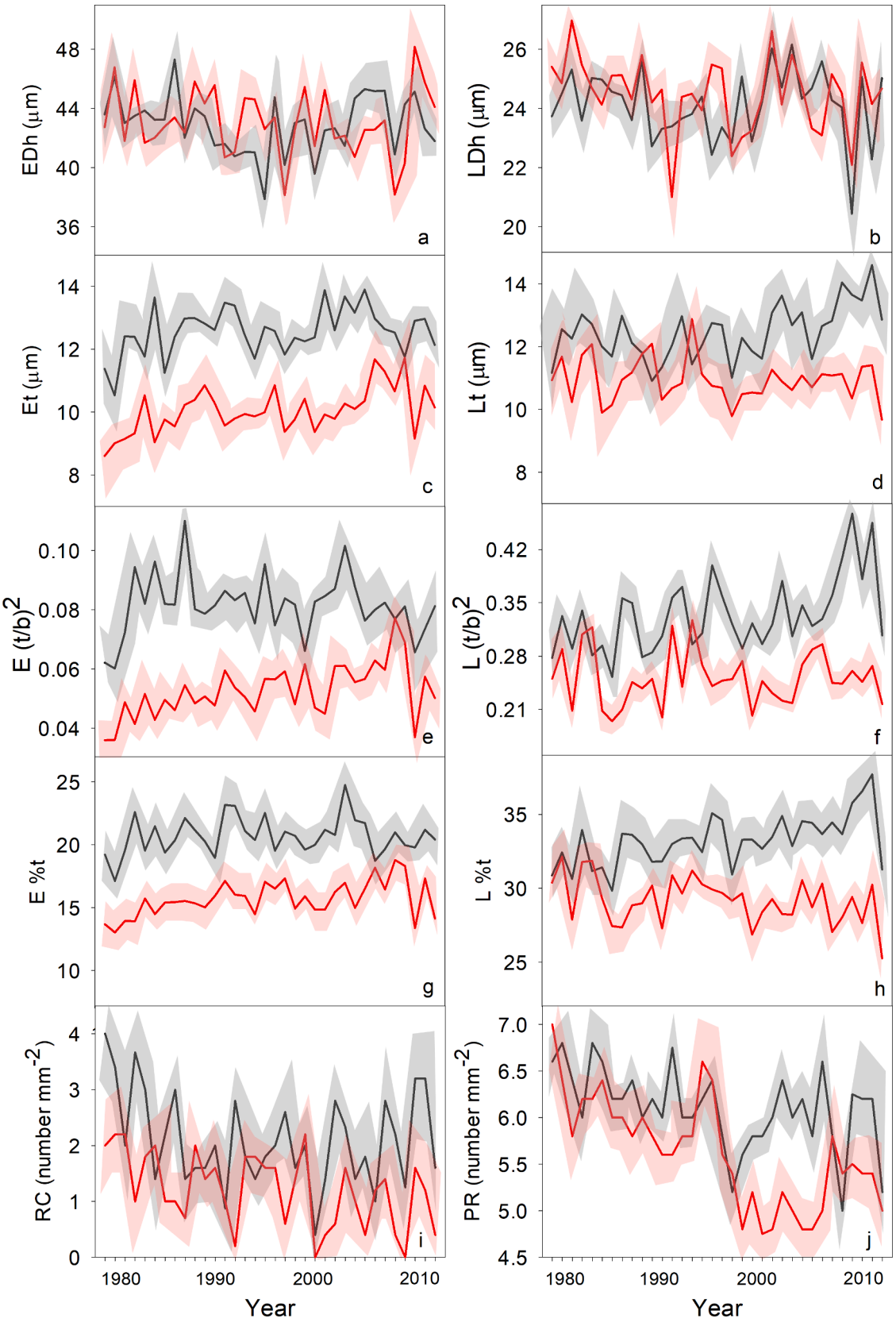

Fig. 3. Wood-anatomical traits of earlywood (E, left panels: a, c, e, g),latewood (L, right panels: b, d, f, h), resin canals and parenchyma rays for living (black lines) and dead (red lines) trees from 1980 to 2013. Abbreviations: E, earlywood; L, latewood; Dh: tracheid hydraulic diameter; t: wall thickness; $(t/b)^2$: thickness to span ratio;%t: percentage of area occupied by cells walls; RC: density of resin canals; PR: density of parenchyma rays. Polygons surrounding the lines represent the standard error. (For interpretation of the references to colour in this figure legend, the reader is referred to the web version of this article.)

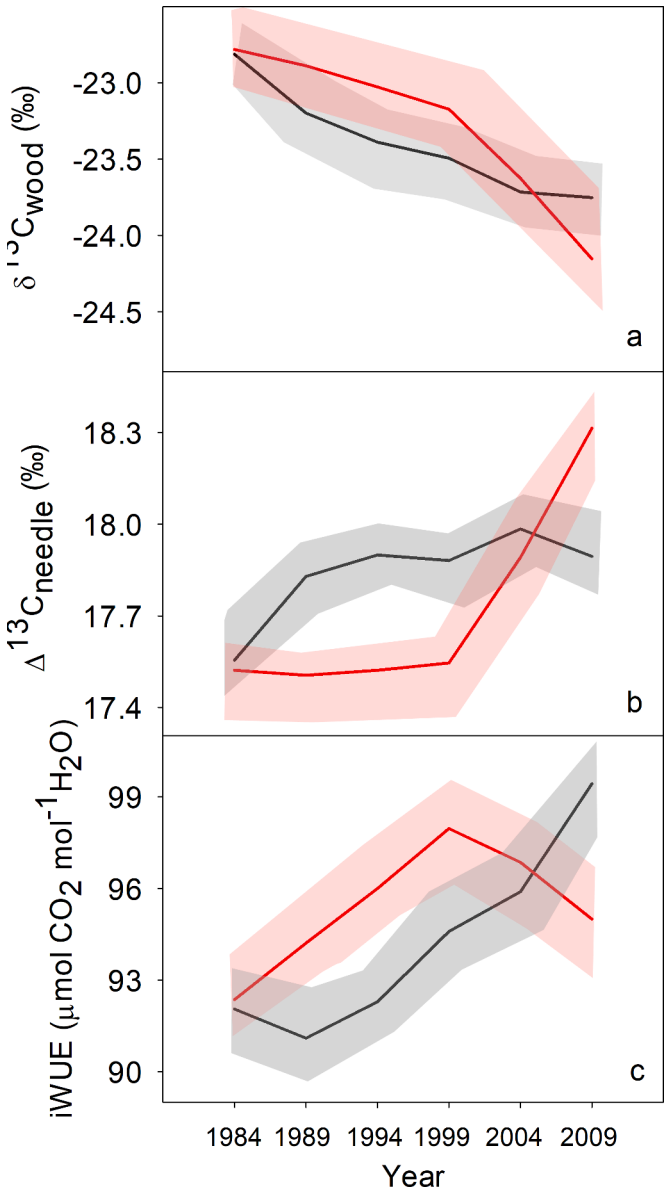

Fig. 4. Raw carbon isotopic composition of tree growth rings ($\delta^{13}C_{wood}$) grouped in 5-year intervals (a), and derived needle carbon isotope discrimination ($\Delta^{13}C$, b) and intrinsic water use efficiency (iWUE, c) in living (black lines) and dead (red lines) trees. Polygons surrounding the lines represent the standard error. (For interpretation of the references to colour in this figure legend, the reader is referred to the web version of this article.)

refilling mechanisms is by growing new xylem tissue (Brodribb et al., 2010). During the production of new conductive tissue under conditions of limited carbon assimilation, some trees ultimately succumb to a depletion of accessible carbon reserves (Trugman et al., 2018). Three results in our study would support a gradual increase of carbon limitation to maintain water transport, storage, and defense in dead trees: lower growth and wood density, fewer parenchyma rays and resin canals, and a sudden change in iWUE, from higher to lower values than in living trees.

The first sign of carbon limitation in dead trees was their consistently lower growth and progressive decrease of latewood density as compared to living trees (Fig. 1; Fig. 2; Fig. S3; Fig. S4). It is a common forester observation that trees that are less vigorous are the first trees to die (Blais, 1958; Parker, 1969). Severe droughts frequently leave persistent legacy effects that progressively decrease growth rates for several years before death (Cailleret et al., 2017). The mechanism by which denser wood is related to drought tolerance is complex. Some studies support the idea that higher wood density is related with the thickness to span ratio of the tracheids or vessels (Fig. 6), thus with greater resistance to implosion (Hacke et al., 2001) and cavitation (Dalla-Salda et al., 2011; Hacke and Sperry, 2001; Hacke et al., 2001; Jacobsen et al., 2007) associated to increasing xylem tension. In some cases, higher tree-ring and latewood densities have been directly related with survival (Martinez-Meier et al., 2008; Ruiz Diaz Britez et al., 2014). Conversely, in other dieback episodes, the lower growth of declining *Abies alba* and *Pinus sylvestris* trees was associated to higher earlywood density and smaller lumen area of earlywood tracheids compared with non-declining trees (Hevia et al., 2019), pointing to a progressive hydraulic impairment under recurrent droughts and increasingly warmer conditions (Pellizzari et al., 2016). After growing in a drought treatment for six years, *Pinus edulis* only produced one or two cell layers of latewood with thinned walls (Sevanto et al., 2018) pointing also to cumulative carbon limitation. In *P. canariensis*, higher density in living trees was not the result of narrower tracheid lumens, and thus of less efficient water transport capacity (Björklund et al., 2017); higher density was the result of thicker walls. Thicker cell walls confer higher resistance to implosion (Hacke and Sperry, 2001), and may have bordered pits less prone to air seeding (Bouche et al., 2014; Delzon et al., 2010). These characteristics make the xylem more resistant to xylem sap tensions but also possibly more expensive to construct in terms of carbon and nutrient costs (Meinzer et al., 2008).

A second evidence of carbon limitation of dead trees was their lower capacity for storage of carbohydrates, nutrients and defense compounds. The density of parenchyma rays decreased in both death and living trees after the 1990s drought, but in the case of dead trees it did not recover afterwards. Since gymnosperms depend on carbohydrate reserves to regrow new xylem after hydraulic failure (Brodribb et al., 2010), the small fraction of parenchyma tissue in dead trees (Fig. 3j) could have compromised their capacity to store and use carbohydrates after the long drought (Rodríguez-Calcerrada et al., 2015). This is particularly true in *P. canariensis* trees, which depend on carbon reserves to resprout and resume growth after disturbances (Miranda et al., 2020). In the same line, fewer resin canals in dead trees, and positive correlation between radial growth and defense traits might reflect a reduced carbon availability to defense (Fig. 3i; Fig. 5; Rodríguez-García et al., 2014; Sala et al., 2010).

A third sign of carbon limitation was the different pattern of iWUE over time between dead and living trees (Fig. 4). The fact that $\Delta^{13}C_{needle}$ increased during 1987- 1991 relative to 1982–1986 in living trees but not in dead trees suggests that Ci/Ca ratio remained constant in dead trees (Linares and Camarero, 2012), which points to persistent water stress and reduced stomatal conductance in dead trees (Cano et al., 2014; Warren et al., 2011). The better water status of living trees could be related with differences in soil and root depth. Any of both factors is in agreement with the positive correlation between winter precipitation and next year radial growth in living trees, whereas dead trees in shallower soils and/or having shallower roots would rely on current-year spring precipitation to sustain radial growth (Table S3).

The low growth rates and possibly reduced stomatal conductance associated to higher iWUE of dead trees during the driest period, from 1991 to 2001, appeared to be efficient in saving water and sustaining hydraulic functions on the short term (López et al., 2021). On the long run, however, stomatal limitations to carbon uptake might cause a progressive decline of the water transport capacity due to reduced growth of new xylem which can compromise water transport in case of significant drought induced embolism after long or intense droughts (Galiano et al., 2011; Gessler et al., 2018).

The iWUE of dead trees dropped sharply and continuously after the dry and warm 1992–2001 decade, and despite the rising atmospheric CO_2 trend (Fig. 4, Table 3). Although a reduction in iWUE (derived from $\delta^{13}C_{wood}$) in mesic trees species suffering die-back from severe droughts has been often related to delayed stomatal closure and increased

Table 3
Measured and estimated values (± SE) of carbon isotope composition ($\delta^{13}C$, ‰) in tree rings and in needles, and discrimination against 13-carbon in the needles ($\Delta^{13}C_{needle}$, ‰) with respect to the air source at each 5-year time period. iWUE (μmol CO_2 mol^{-1} H_2O) for dead and living trees was derived form $\Delta^{13}C_{needle}$ using equation (3) described in the main text.

Period	$\delta^{13}C_{wood}$ (‰) Living	$\delta^{13}C_{wood}$ (‰) Dead	$\delta^{13}C_{needle}$ (‰) Living	$\delta^{13}C_{needle}$ (‰) Dead	$\delta^{13}C_{atmos}$ (‰)	$[CO_2]$ atm (ppm)	$\Delta^{13}C_{needle}$(‰) Living	$\Delta^{13}C_{needle}$(‰) Dead	iWUE (μmol CO_2 mol^{-1} H_2O) Living	iWUE (μmol CO_2 mol^{-1} H_2O) Dead
2011–2007	−23.75 (0.25)	−24.15 (0.28)	−25.75 (0.25)	−26.15 (0.28)	−8.32	387.34	17.89 (0.09)	18.31 (0.12)	99.43 (1.81)	94.99 (1.54)
2006–2002	−23.72 (0.25)	−23.63 (0.25)	−25.72 (0.25)	−25.63 (0.25)	−8.19	377.18	17.98 (0.11)	17.89 (0.16)	95.89 (1.78)	96.86 (1.86)
2001–1997	−23.49 (0.20)	−23.17 (0.25)	−25.49 (0.20)	−25.17 (0.25)	−8.07	367.97	17.88 (0.10)	17.55 (0.14)	94.59 (1.72)	97.96 (1.81)
1996–1992	−23.39 (0.25)	−23.03 (0.28)	−25.39 (0.25)	−25.03 (0.28)	−7.94	359.72	17.90 (0.09)	17.52 (0.12)	92.29 (1.40)	96.00 (1.60)
1991–1987	−23.20 (0.25)	−22.89 (0.20)	−25.20 (0.25)	−24.89 (0.20)	−7.82	352.43	17.83 (0.09)	17.51 (0.10)	91.10 (1.30)	94.21 (1.42)
1986–1982	−22.81 (0.20)	−22.78 (0.20)	−24.81 (0.20)	−24.78 (0.20)	−7.69	346.09	17.55 (0.10)	17.52 (0.10)	92.05 (1.32)	92.36 (1.32)

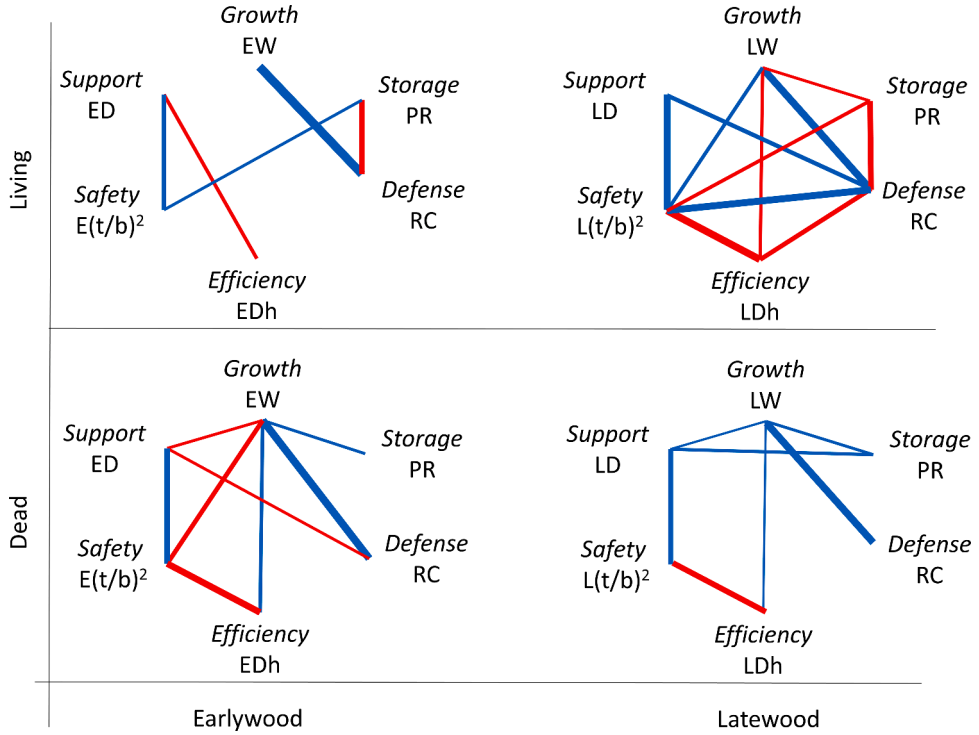

Fig. 5. Xylem function correlations for earlywood (left) and latewood (right) of living (upper) and dead (lower) trees. Blue lines show positive correlations and red lines show negative correlations. Correlation strength is represented by line thickness Only significant correlations are shown ($P < 0.05$). See Table 1 for definition of traits and abbreviations of variables. (For interpretation of the references to colour in this figure legend, the reader is referred to the web version of this article.)

hydraulic failure risk (Hentschel et al., 2014; Petrucco et al., 2017), this behavior is unlike to happened in a pine species adapted to arid environments, such as *P. canariensis* (Brito et al., 2016). Instead, the drop of iWUE (and concomitant increase in $^{13}CO_2$ discrimination), also found in other drought-declined trees (Linares and Camarero, 2012), may reflect limited carboxylation (Warren et al., 2011; Cano et al., 2014). As $\delta^{13}C_{wood}$ was the only source of variation in iWUE among living and dead trees represented in the simplified model for $\Delta^{13}C_{needle}$ (see eq. (3)), any process that affected post photosynthetic carbon discrimination differentially in dead and in living trees could have changed $\delta^{13}C_{wood}$, although not necessarily iWUE. We identify two complementary processes that may reduce $\delta^{13}C_{wood}$ independently of iWUE that point also to higher cumulative water stress in dead trees: i) higher use of ^{13}C-enriched carbohydrate reserves synthesized in more humid years to build-up new tracheid cell walls due to a decline in recent photosynthates (Brüggemann et al., 2011; Sarris et al., 2013), and ii) a reduction in the ratio of ^{13}C-enriched cellulose/hemicellulose to lignin (Loader et al., 2003). However, both processes are unlikely to explain differences in $\delta^{13}C_{wood}$ between living and dead trees because, on one hand, most of carbon reserves would have been consumed by the time of death (2013) and, on the other hand tree ring density (and likey lignin synthesis) decreased over time in dead trees (Fig. 2).

4.2. Phenotypic integration and climate imprints on the xylem of living and dead trees

The effectiveness of xylem adjustments in long term drought acclimation is limited by the activity of the cambium and by trade-offs between xylem functions. Cambium phenology of living and dead trees seemed to be differentially affected by climate. In living trees,

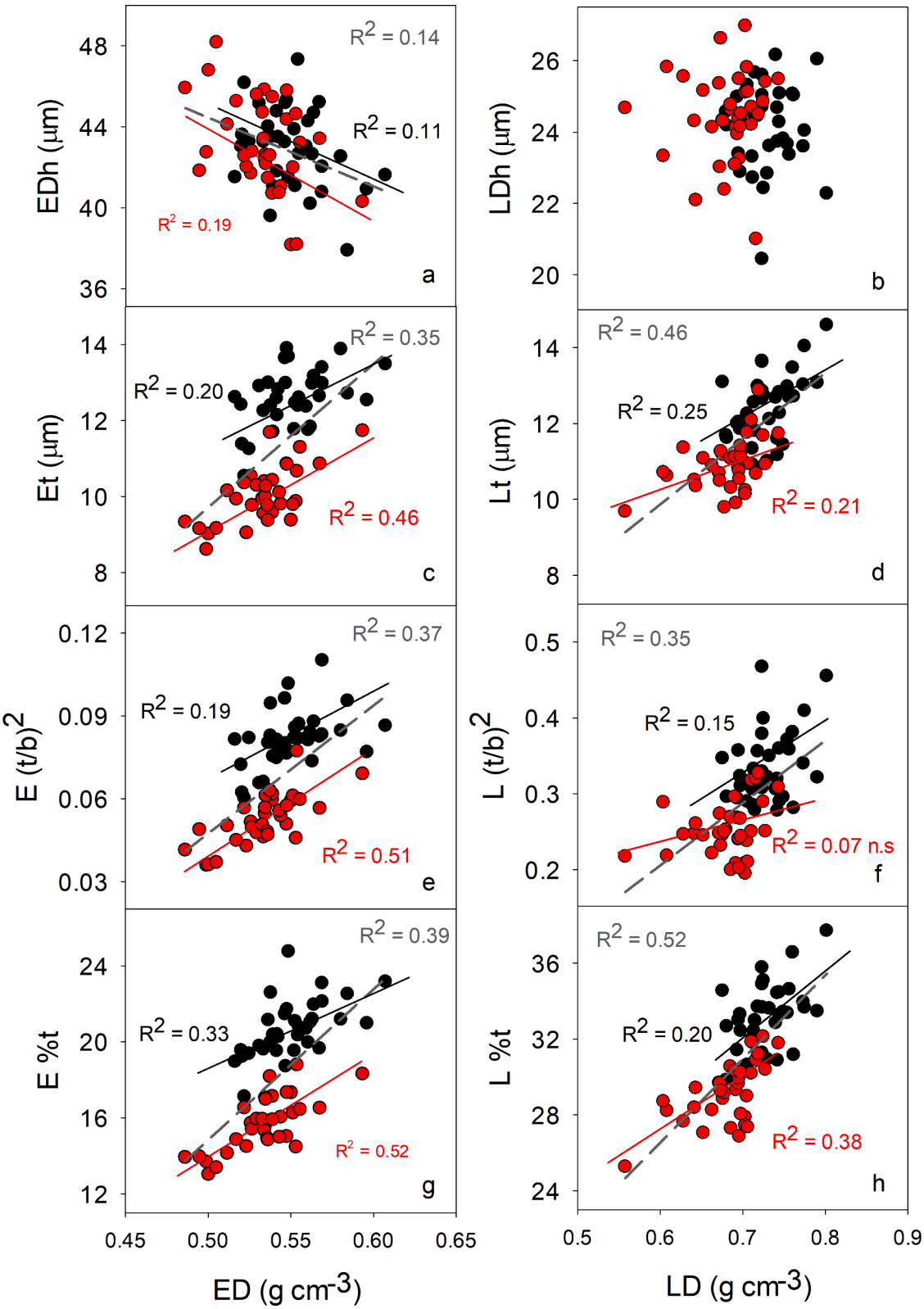

Fig. 6. Regression lines between earlywood density (ED; left panels) and latewood density (LD; right panels) and anatomical traits considering living (black symbols) and dead (red symbols) trees. Dashed gray lines correspond to the regression lines pooling living and dead trees (corresponding regression coefficients appear in gray). Dh: tracheid hydraulic diameter; t: wall thickness; $(t/b)^2$: thickness to span ratio;%t: percentage of area occupied by walls; n.s.: non-significant. (For interpretation of the references to colour in this figure legend, the reader is referred to the web version of this article.)

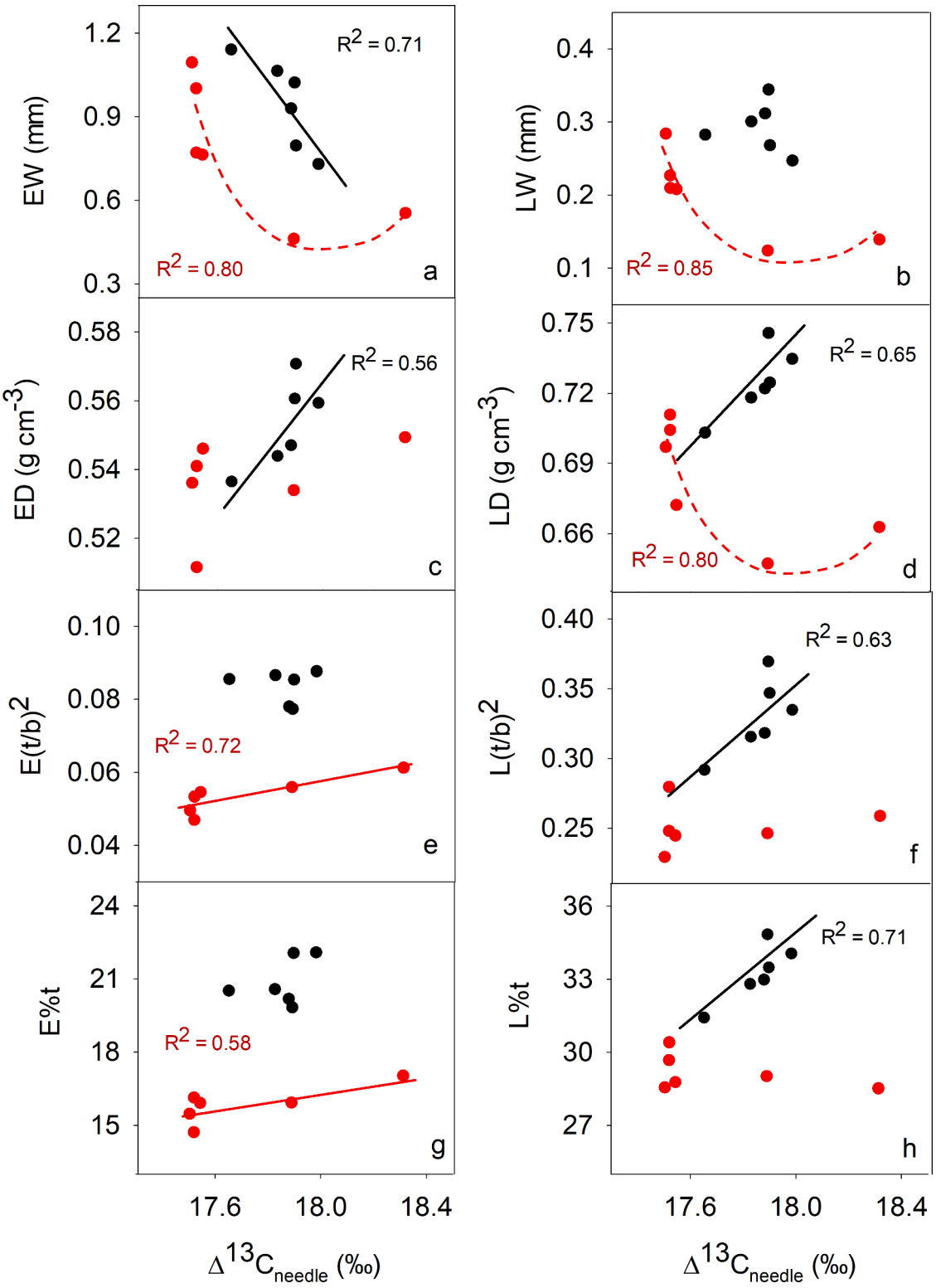

Fig. 7. Correlations between $\Delta^{13}C$ and anatomical traits considering living (black symbols) and dead (red symbols) trees. Linear regressions are shown with full lines and nonlinear regressions with dashed lines. Abbreviations: EW: earlywood width; LW: latewood width; ED: earlywood density; LD: latewood density; $E(t/b)^2$: earlywood thickness to span ratio; $L(t/b)^2$: latewood thickness to span ratio; E%t: percentage of xylem area occupied by walls in the earlywood; L%t: percentage of xylem area occupied by walls in the latewood. (For interpretation of the references to colour in this figure legend, the reader is referred to the web version of this article.)

earlywood growth and earlywood hydraulic efficiency relied on precipitation of the previous winter, pointing to stored water in deep soil layers, and stored photosynthates as crucial for radial growth at the beginning of the growing season (Gessler et al., 2009; Rathgeber, 2017; Rodríguez-García et al., 2015). Conversely, earlywood growth of dead trees was more sensitive to spring climate (Table S3), which could be due to shallower soils and/or roots. Latewood water transport efficiency and density, however, were more influenced by spring and summer precipitation in living trees and by autumn precipitation in dead trees (Table S3). This suggests that a significant amount of the carbon used for cell-wall formation in the latewood was captured earlier in the growing season in living trees than in dead ones, which may be crucial for survival of *P. canariensis* under conditions of severe summer drought (Brito et al., 2010). Only if water availability in autumn increases, *P. canariensis* can resume growth and use the carbon accumulated previously for latewood formation (Brito et al., 2016). Thus, a progressive decline in reserves induced by drought or any other stress can make trees more sensitive to water shortage and more likely to die from sustained and/or severe climatic anomalies.

Two positive correlations between xylem functions were observed for both earlywood and latewood of dead and living trees; one between support and water transport safety, and other between growth and defense. In conifers, both canopy support and implosion resistance require high carbon investment in tracheid cell walls, which increases wood density and in turn decreases water transport efficiency (Fig. 5; Hacke et al., 2001; Pittermann et al., 2006; Sperry et al., 2006). The positive correlation between growth and density of resin canals would reflect the dependence of the defense system on the size and mobilization of carbon stocks (Rodríguez-García et al., 2014). Other correlations differed, though, between living and dead trees. In dead trees, wider growth rings showed a more efficient but less safe and dense earlywood xylem (Fig. 5; Zadworny et al., 2019). Lower values of $\Delta^{13}C_{needle}$ were associated with lower wood density, lower resistance to implosion and lower proportion of cell walls in the latewood of living trees but in the earlywood of dead trees (Fig. 7), reinforcing the hypothesis of a differential phenology and use of water and carbon reserves between dead and living trees. All together these results suggest that living trees responded to increasing summer drought by producing a particular type of latewood, denser and more resistant to implosion than that of dead trees. This distinctive response lasted over several years after the 1990s drought, and was not restricted to punctual annual events. Dead trees survived the decade-long drought but remained permanently affected and could not fully recover xylem functionality, suffering a progressive decline in latewood density, which rendered them more sensitive to the severe drought of 2011–2012. Differences between dead and living trees might be genetic but we cannot discard that differences in rooting depth due to microsite conditions were ultimately responsible of differences in vigor (Petrucco et al., 2017).

5. Conclusions

We show that tree mortality in an arid environment was preceded by lower growth, wood density and iWUE. These results can be used to forecast mortality in drought-prone environments using tree cores, and to retrospectively infer the physiological mechanisms involved. Moreover, our data suggest that even if trees can suffer from carbon limitation during decades (as inferred from thinner tracheid cell walls and decreasing latewood density), the ultimate cause of death after a severe drought seems to be a generalized failure of a progressively weaker plant hydraulic system.

Declaration of Competing Interest

The authors declare that they have no known competing financial interests or personal relationships that could have appeared to influence the work reported in this paper.

Acknowledgements

We are grateful to the Canary Islands Government and the Cabildo of Gran Canaria, particularly to Carlos Velázquez who has supported our work in Gran Canaria for many years. We would like to thank Frédéric Millier for helping us with sample preparation and the X-ray microdensity profiles. This work was supported by the Spanish Ministry of Science in the Project AGL2009–10606 (VULCAN) and by a short stay of RL in Orleans funded by the COST action STReESS (COST-FP1106).

Supplementary materials

Supplementary material associated with this article can be found, in the online version, at doi:10.1016/j.agrformet.2021.108634.

References

Adams, H.D., et al., 2017. A multi-species synthesis of physiological mechanisms in drought-induced tree mortality. Nat. Ecol. Evol. 1 (9), 1285–1291.
Allen, C.D., Breshears, D.D., McDowell, N.G., 2015. On underestimation of global vulnerability to tree mortality and forest die-off from hotter drought in the. Anthropocene. Ecosphere 6 (8), art129.
Allen, C.D., et al., 2010. A global overview of drought and heat-induced tree mortality reveals emerging climate change risks for forests. For. Ecol. Manage. 259 (4), 660–684.
Battipaglia, G., et al., 2013. Elevated CO 2 increases tree-level intrinsic water use efficiency: insights from carbon and oxygen isotope analyses in tree rings across three forest FACE sites. New Phytol. 197 (2), 544–554.
Bigler, C., Veblen, T.T., 2009. Increased early growth rates decrease longevities of conifers in subalpine forests. Oikos 118 (8), 1130–1138.
Björklund, J., et al., 2017. Cell size and wall dimensions drive distinct variability of earlywood and latewood density in northern hemisphere conifers. New Phytol. 216 (3), 728–740.
Blais, J., 1958. The vulnerability of balsam fir to spruce budworm attack in northwestern Ontario, with special reference to the physiological age of the tree. The For. Chronicle 34 (4), 405–422.
Bose, A.K., et al., 2020. Growth and resilience responses of Scots pine to extreme droughts across Europe depend on pre-drought growth conditions. Glob. Chang. Biol.
Bouche, P.S., et al., 2014. A broad survey of hydraulic and mechanical safety in the xylem of conifers. J. Exp. Bot. 65 (15), 4419–4431.
Brito, P., et al., 2016. Increased water use efficiency does not prevent growth decline of pinus canariensis in a semi-arid treeline ecotone in tenerife, canary islands (Spain). Ann. For. Sci. 73 (3), 741–749.
Brito, P., Morales, D., Wieser, G., Jiménez, M.S., 2010. Spatial and seasonal variations in stem CO 2 efflux of pinus canariensis at their upper distribution limit. Trees 24 (3), 523–531.
Brodribb, T.J., Bowman, D.J., Nichols, S., Delzon, S., Burlett, R., 2010. Xylem function and growth rate interact to determine recovery rates after exposure to extreme water deficit. New. Phytol. 188 (2), 533–542.
Brüggemann, N., et al., 2011. Carbon allocation and carbon isotope fluxes in the plant-soil-atmosphere continuum: a review. Biogeosciences 8 (11), 3457–3489.
Burnham, K.P., Anderson, D.R., 2002. A Practical Information-Theoretic approach. Model selection and Multimodel Inference, 2nd ed. Springer, New York, p. 2.
Cailleret, M., et al., 2017. A synthesis of radial growth patterns preceding tree mortality. Glob. Chang. Biol. 23 (4), 1675–1690.
Camarero, J.J., Gazol, A., Sangüesa-Barreda, G., Oliva, J., Vicente-Serrano, S.M., 2015a. To die or not to die: early warnings of tree dieback in response to a severe drought. J. Ecol. 103 (1), 44–57.
Camarero, J.J., Gazol, A., Tardif, J.C., Conciatori, F., 2015b. Attributing forest responses to global-change drivers: limited evidence of a CO2-fertilization effect in iberian pine growth. J. Biogeogr. 42 (11), 2220–2233.
Cano, F.J., López, R., Warren, C.R., 2014. Implications of the mesophyll conductance to CO2 for photosynthesis and water-use efficiency during long-term water stress and recovery in two contrasting eucalyptus species. Plant. Cell. Environ. 37 (11), 2470–2490.
Choat, B., et al., 2018. Triggers of tree mortality under drought. Nature 558 (7711), 531–539.
Dai, A., 2013. Increasing drought under global warming in observations and models. Nat. Clim. Chang. 3 (1), 52–58.
Dalla-Salda, G., et al., 2014. Dynamics of cavitation in a Douglas-fir tree-ring: transition-wood, the lord of the ring? Journal of Plant Hydraulics 1, 005.
Dalla-Salda, G., Martinez-Meier, A., Cochard, H., Rozenberg, P., 2011. Genetic variation of xylem hydraulic properties shows that wood density is involved in adaptation to drought in Douglas-fir (Pseudotsuga menziesii (Mirb.)). Ann. For. Sci. 68 (4), 747–757.
Delzon, S., Douthe, C., Sala, A., Cochard, H., 2010. Mechanism of water-stress induced cavitation in conifers: bordered pit structure and function support the hypothesis of seal capillary-seeding. Plant Cell Environ. 33 (12), 2101–2111.
DeSoto, L., et al., 2020. Low growth resilience to drought is related to future mortality risk in trees. Nat. Commun. 11 (1), 1–9.

Dlugokencky, E.J., J.W. Mund, A.M. Crotwell, M.J. Crotwell, and K.W. Thoning (2019), Atmospheric carbon dioxide dry air mole fractions from the NOAA ESRL carbon cycle cooperative global air sampling network, 1968-2018, Version: 2019-07, doi:10.15138/wkgj-f215.
Domec, J.C., Gartner, B.L., 2002b. How do water transport and water storage differ in coniferous earlywood and latewood? J. Exp. Bot. 53 (379), 2369–2379.
Evans, J., Sharkey, T., Berry, J., Farquhar, G., 1986. Carbon isotope discrimination measured concurrently with gas exchange to investigate CO2 diffusion in leaves of higher plants. Funct. Plant Biol. 13 (2), 281–292.
Farquhar, G., Richards, R., 1984. Isotopic composition of plant carbon correlates with water-use efficiency of wheat genotypes. Funct. Plant Biol. 11 (6), 539–552.
Farquhar, G.D., O'Leary, M.H., Berry, J.A., 1982. On the relationship between carbon isotope discrimination and the intercellular carbon dioxide concentration in leaves. Funct. Plant Biol. 9 (2), 121–137.
Ferrio, J., Voltas, J., 2005. Carbon and oxygen isotope ratios in wood constituents of Pinus halepensis as indicators of precipitation, temperature and vapour pressure deficit. Tellus B: Chemical and Physical Meteorology 57 (2), 164–173.
Fonti, P., et al., 2010. Studying global change through investigation of the plastic responses of xylem anatomy in tree rings. New. Phytol. 185 (1), 42–53.
Francey, R., Farquhar, G., 1982. An explanation of 13 C/12 C variations in tree rings. Nat. 297 (5861), 28–31.
Francey, R., Gifford, R., Sharkey, T., Weir, B., 1985. Physiological influences on carbon isotope discrimination in huon pine (Lagarostrobos franklinii). Oecologia 66 (2), 211–218.
Galiano, L., Martínez-Vilalta, J., Lloret, F., 2011. Carbon reserves and canopy defoliation determine the recovery of Scots pine 4yr after a drought episode. New Phytol. 190 (3), 750–759.
Garcia-Forner, N., Sala, A., Biel, C., Savé, R., Martínez-Vilalta, J., 2016. Individual traits as determinants of time to death under extreme drought in Pinus sylvestris L. Tree Physiol. 36 (10), 1196–1209.
Gessler, A., et al., 2009. Tracing carbon and oxygen isotope signals from newly assimilated sugars in the leaves to the tree-ring archive. Plant Cell Environ. 32 (7), 780–795.
Gessler, A., et al., 2018. Drought induced tree mortality – a tree-ring isotope based conceptual model to assess mechanisms and predispositions. New Phytol. 219 (2), 485–490.
Granda, E., Rossatto, D.R., Camarero, J.J., Voltas, J., Valladares, F., 2014. Growth and carbon isotopes of Mediterranean trees reveal contrasting responses to increased carbon dioxide and drought. Oecologia 174 (1), 307–317.
Hacke, U.G., Sperry, J.S., 2001. Functional and ecological xylem anatomy. Perspect. Plant Ecol., Evolution and Systematics, 4 (2), 97–115.
Hacke, U.G., Sperry, J.S., Pockman, W.T., Davis, S.D., McCulloh, K.A., 2001. Trends in wood density and structure are linked to prevention of xylem implosion by negative pressure. Oecologia 126 (4), 457–461.
Hacke, U.G., Sperry, J.S., Wheeler, J.K., Castro, L., 2006. Scaling of angiosperm xylem structure with safety and efficiency. Tree Physiol. 26 (6), 689–701.
Hampe, A., Petit, R.J., 2005. Conserving biodiversity under climate change: the rear edge matters. Ecol. Lett. 8 (5), 461–467.
Hentschel, R., et al., 2014. Norway spruce physiological and anatomical predisposition to dieback. For. Ecol. Manage. 322, 27–36.
Heres, A.-.M., Martínez-Vilalta, J., López, B.C., 2012. Growth patterns in relation to drought-induced mortality at two scots pine (Pinus sylvestris L.) sites in NE iberian peninsula. Trees 26 (2), 621–630.
Hevia, A., et al., 2019. Long-term nutrient imbalances linked to drought-triggered forest dieback. Sci. Total Environ. 690, 1254–1267.
Jacobsen, A.L., Pratt, R.B., Ewers, F.W., Davis, S.D., 2007. Cavitation resistance among 26 chaparral species of southern California. Ecol. Monogr. 77 (1), 99–115.
Linares, J.C., Camarero, J.J., 2012. From pattern to process: linking intrinsic water-use efficiency to drought-induced forest decline. Glob. Chang. Biol. 18 (3), 1000–1015.
Loader, N., Robertson, I., McCarroll, D., 2003. Comparison of stable carbon isotope ratios in the whole wood, cellulose and lignin of oak tree-rings. Palaeogeography, Palaeoclimatology, Palaeoecology, 196 (3–4), 395–407.
López de Heredia, U., López, R., Collada, C., Emerson, B.C., Gil, L., 2014. Signatures of volcanism and aridity in the evolution of an insular pine (Pinus canariensis Chr. Sm. Ex DC in Buch). Heredity 113 (3), 240–249.
López, R., Zehavi, A., Climent, J., Gil, L, 2007. Contrasting ecotypic differentiation for growth and survival in Pinus canariensis. Aust. J. Bot. 55 (7), 759–769.
López, R., Climent, J., Gil, L, 2008. From desert to cloud forest: the non-trivial phenotypic variation of Canary Island pine needles. Trees 22 (6), 843–849.
López, R., Climent, J., Gil, L, 2010. Intraspecific variation and plasticity in growth and foliar morphology along a climate gradient in the Canary Island pine. Trees 24 (2), 343–350.
López, R., Cano, F.J., Choat, B., Cochard, H., Gil, L., 2016. Plasticity in vulnerability to cavitation of pinus canariensis occurs only at the driest end of an aridity gradient. Front Plant Sci. 7.
López, R., Cano, F.J., Martin-StPaul, N.K., Cochard, H., Choat, B., 2021. Coordination of stem and leaf traits define different strategies to regulate water loss and tolerance ranges to aridity. New Phytol. https://doi.org/10.1111/nph.17185.
López, R., et al., 2013. Vulnerability to cavitation, hydraulic efficiency, growth and survival in an insular pine (Pinus canariensis). Ann. Bot. 111 (6), 1167–1179.
Martinez-Meier, A., Sanchez, L., Pastorino, M., Gallo, L., Rozenberg, P., 2008. What is hot in tree rings? The wood density of surviving Douglas-firs to the 2003 drought and heat wave. For. Ecol. Manage. 256 (4), 837–843.
Martínez-Vilalta, J., 2018. The rear window: structural and functional plasticity in tree responses to climate change inferred from growth rings. Tree Physiol. 38 (2), 155–158.
McDowell, N., et al., 2008. Mechanisms of plant survival and mortality during drought: why do some plants survive while others succumb to drought? New Phytol. 178 (4), 719–739.
McDowell, N.G., 2011. Mechanisms linking drought, hydraulics, carbon metabolism, and vegetation mortality. Plant Physiol. 155 (3), 1051–1059.
Meinzer, F.C., et al., 2008. Constraints on physiological function associated with branch architecture and wood density in tropical forest trees. Tree Physiol. 28 (11), 1609–1617.
Miranda, J.C., Rodrguez-Calcerrada, J., Pita, P., , et al.O'Grady, A.P., Tissue, D.T., Worledge, D., Pinkard, E.A., 2020. Carbohydrate dynamics in a resprouting species after severe aboveground perturbations. Eur J Forest Res. 139, 841–852. https://doi.org/10.1007/s10342-020-01288-2.
Mitchell, P.J., O'Grady, A.P., Tissue, D.T., Worledge, D., Pinkard, E.A., 2014. Co-ordination of growth, gas exchange and hydraulics define the carbon safety margin in tree species with contrasting drought strategies. Tree Physiol. 34 (5), 443–458.
O'Leary, M.H., 1981. Carbon isotope fractionation in plants. Phytochemistry 20 (4), 553–567.
Parker, J., 1969. Further studies of drought resistance in woody plants. The Botanical Rev. 35 (4), 317–371.
Pellizzari, E., Camarero, J.J., Gazol, A., Sangüesa-Barreda, G., Carrer, M., 2016. Wood anatomy and carbon-isotope discrimination support long-term hydraulic deterioration as a major cause of drought-induced dieback. Glob. Chang. Biol. 22 (6), 2125–2137.
Petrucco, L., Nardini, A., Von Arx, G., Saurer, M., Cherubini, P., 2017. Isotope signals and anatomical features in tree rings suggest a role for hydraulic strategies in diffuse drought-induced die-back of Pinus nigra. Tree Physiol. 37 (4), 523–535.
Pittermann, J., Sperry, J.S., Wheeler, J.K., Hacke, U.G., Sikkema, E.H., 2006. Mechanical reinforcement of tracheids compromises the hydraulic efficiency of conifer xylem. Plant Cell Environ. 29 (8), 1618–1628.
Polge, H., 1966. Établissement des courbes de variation de la densité du bois par exploration densitométrique de radiographies d'échantillons prélevés à la tarière sur des arbres vivants : applications dans les domaines Technologique et Physiologique. Annales des sci. forestières 23 (1). I-206.
Rathgeber, C.B., 2017. Conifer tree-ring density inter-annual variability–anatomical, physiological and environmental determinants. New Phytol. 216 (3), 621–625.
Rodríguez-Calcerrada, J., et al., 2015. Stem CO2 efflux in six co-occurring tree species: underlying factors and ecological implications. Plant Cell Environ. 38 (6), 1104–1115.
Rodríguez-Calcerrada, J., et al., 2017a. Drought-Induced Oak Decline—Factors Involved, Physiological Dysfunctions, and Potential Attenuation by Forestry Practices. Editors. In: Gil-Pelegrín, E., Peguero-Pina, J.J., Sancho-Knapik, D. (Eds.), Oaks Physiological Ecology. Exploring the Functional Diversity of Genus Quercus L. Springer International Publishing, Cham, pp. 419–451.
Rodríguez-Calcerrada, J., et al., 2017b. Drought-induced shoot dieback starts with massive root xylem embolism and variable depletion of nonstructural carbohydrates in seedlings of two tree species. New Phytol. 213 (2), 597–610.
Rodríguez-García, A., López, R., Martín, J.A., Pinillos, F., Gil, L., 2014. Resin yield in Pinus pinaster is related to tree dendrometry, stand density and tapping-induced systemic changes in xylem anatomy. For. Ecol. Manage. 313, 47–54.
Rodríguez-García, A., et al., 2015. Influence of climate variables on resin yield and secretory structures in tapped Pinus pinaster. Ait. in central Spain. Agric. For. Meteorol. 202, 83–93.
Rodríguez-García, A., Martín, J.A., López, R., Sanz, A., Gil, L., 2016. Effect of four tapping methods on anatomical traits and resin yield in Maritime pine (Pinus pinaster Ait.). Ind. Crops Prod. 86, 143–154.
Ruiz Diaz Britez, M., Sergent, A.-.S., Martinez Meier, A., Bréda, N., Rozenberg, P., 2014. Wood density proxies of adaptive traits linked with resistance to drought in Douglas fir (Pseudotsuga menziesii (Mirb.) Franco). Trees 28 (5), 1289–1304.
Sala, A., Piper, F., Hoch, G., 2010. Physiological mechanisms of drought-induced tree mortality are far from being resolved. New Phytol. 186 (2), 274–281.
Sánchez-Salguero, R., et al., 2017. Assessing forest vulnerability to climate warming using a process-based model of tree growth: bad prospects for rear-edges. Glob. Chang. Biol. 23 (7), 2705–2719.
Sarris, D., Siegwolf, R., Körner, C., 2013. Inter- and intra-annual stable carbon and oxygen isotope signals in response to drought in Mediterranean pines. Agric. For. Meteorol. 168, 59–68.
Sass-Klaassen, U., et al., 2016. A tree-centered approach to assess impacts of extreme climatic events on forests. Front. Plant Sci. 7, 1069.
Seibt, U., Rajabi, A., Griffiths, H., Berry, J.A., 2008. Carbon isotopes and water use efficiency: sense and sensitivity. Oecologia 155 (3), 441.
Sevanto, S., Mcdowell, N.G., Dickman, L.T., Pangle, R., Pockman, W.T., 2014. How do trees die? A test of the hydraulic failure and carbon starvation hypotheses. Plant Cell Environ. 37 (1), 153–161.
Sperry, J.S., Hacke, U.G., Pittermann, J., 2006. Size and function in conifer tracheids and angiosperm vessels. Am. J. Bot. 93 (10), 1490–1500.
Staley, J.M., 1965. Decline and mortality of red and scarlet oaks. For. Sci. 11 (1), 2–17.
Trugman, A., et al., 2018. Tree carbon allocation explains forest drought-kill and recovery patterns. Ecol. Lett. 21 (10), 1552–1560.
Tyree, M.T., Zimmermann, M.H., 2002. Hydraulic Architecture of Whole Plants and Plant performance, Xylem structure and the Ascent of Sap. Springer, pp. 175–214.
Voltas, J., et al., 2013. A retrospective, dual-isotope approach reveals individual predispositions to winter-drought induced tree dieback in the southernmost distribution limit of Scots pine. Plant Cell Environ. 36 (8), 1435–1448.
Warren, C.R., Aranda, I., Cano, F.J., 2011. Responses to water stress of gas exchange and metabolites in Eucalyptus and Acacia spp. Plant Cell Environ. 34 (10), 1609–1629.

Wood, S.N., 2003. Thin plate regression splines. J. R. Stat. Soc.: Series B (Stat. Methodol.) 65 (1), 95–114.
Wood, S.N., 2017. Generalized Additive models: an Introduction With R. CRC press.
Zadworny, M., et al., 2019. Regeneration origin affects radial growth patterns preceding oak decline and death–insights from tree-ring δ13C and δ18O. Agric. For. Meteorol. 278, 107685.